Polaron hopping conduction and thermoelectric power in LaMnO 3+δ

Sudipta Pal, Aritra Banerjee, E. Rozenberg, and B. K. Chaudhuri

Citation: Journal of Applied Physics **89**, 4955 (2001); doi: 10.1063/1.1362411
View online: http://dx.doi.org/10.1063/1.1362411
View Table of Contents: http://scitation.aip.org/content/aip/journal/jap/89/9?ver=pdfcov
Published by the AIP Publishing

Polaron hopping conduction and thermoelectric power in $LaMnO_{3+\delta}$

Sudipta Pal, Aritra Banerjee, E. Rozenberg,[a] and B. K. Chaudhuri[b]
Solid State Physics Department, Indian Association for the Cultivation of Science, Calcutta-700032, India

(Received 21 July 2000; accepted for publication 14 February 2001)

Two different phases of $LaMnO_{3+\delta}$ [one showing a metal–insulator transition (MIT), referred to as LaMn–C, and the other not showing a MIT, referred to as LaMn-S] have been clearly observed to follow two different conduction mechanisms. Interestingly, small polaron hopping models of Mott, Schnakenberg, and Emin are found to fit the conductivity data of all the samples above the corresponding MIT temperature. The conductivity data of the insulating (semiconducting) LaMn–S followed a nonadiabatic hopping conduction mechanism while LaMn–C and the Pb doped samples viz. $La_{1-x}Pb_xMnO_3$ ($x=0.05-0.5$) showed a similar type of MIT and followed an adiabatic small polaron hopping conduction mechanism in the high temperature paramagnetic phase (above the respective MIT temperature). Activation energy (W), density of states at the Fermi level $N(E_F)$, Debye temperature (θ_D), electron–phonon interaction constant (γ_P), etc. of LaMn–S showed appreciable differences from those of LaMn–C and $La_{1-x}Pb_xMnO_3$, which show a MIT. Polaron hopping conduction is also supported by thermoelectric power (TEP) measurements. An observed small but appreciable magnetic field dependence of the TEP data (measured at $B=1.5$ T) is considered to be associated with magnetic polarons. © *2001 American Institute of Physics.* [DOI: 10.1063/1.1362411]

I. INTRODUCTION

$LaMnO_{3+\delta}$ is one of the widely studied materials of current interest showing semiconductor to metal transition and giant magnetoresistance peak around room temperature when La is partially replaced by a divalent element like Ca, Ba, Sr, Pb, etc.[1–8] However, the conduction mechanism in such mixed valence materials is a complex interplay between magnetic spin, charge ordering, and also structural change. The $LaMnO_{3+\delta}$ oxide contains both Mn^{3+} and Mn^{4+} ions and with a small portion of Mn^{4+} (<5%), it becomes antiferromagnetically ordered at low temperature (~150 K). When La^{3+} is progressively substituted by a divalent cation, it becomes ferromagnetic with a well defined Curie temperature (T_C), and metallic below T_C. Zener[9] proposed that magnetism in such a system is primarily caused by a double exchange mechanism. The basic process in the double exchange is the hopping of d hole from $Mn^{4+}(d^3,t_{2g}^3,S=3/2)$ to $Mn^{3+}(d^4,t_{2g}^3,e_g',S=2)$ via oxygen (Mn^{4+}–O–Mn^{3+}), so that Mn^{4+} and Mn^{3+} ion exchange takes place. Therefore, polaronic hopping conduction mechanism is responsible for the conducting behavior of this system. The Mn^{4+}–O–Mn^{3+} superexchange interaction in $LaMnO_3$ is ferromagnetic while Mn^{3+}–O–Mn^{3+} and Mn^{4+}–O–Mn^{4+} interaction is antiferromagnetic. Since lattice interaction is also involved, there is strong electron (hole)–phonon interaction in such compounds above the metal–insulator transition (MIT). Such strong electron–lattice (phonon) interaction leads to the polaron formation.[10,11] Recently small-polaron transport mechanism was also applied to fit the conductivity and thermoelectric power of the Zn doped $Fe_{1-x}Zn_xCr_2S_4$ showing[12] colossal magnetoresistance. It is also known that polarons have been studied both in ordered[13] and disordered[14] solids.

In this article, we report the transport mechanism in the two similar phases of $LaMnO_{3+\delta}$ (one showing MIT, referred to as LaMn–C and the other not showing MIT referred to as LaMn–S) using small polaron hopping models.[10,11] To compare the properties of LaMn–C with similar other doped manganite samples showing MIT, we also prepared and studied a typical Pb doped system viz. $La_{1-x}Pb_xMnO_3$ ($x=0.05-0.5$). Since all the Pb doped samples showed similar transport behavior, we report here the properties of $La_{0.9}Pb_{0.1}MnO_3$ only (hereafter referred to as LaPbMn–C). Thermoelectric power (TEP) of the samples, in the absence and presence of magnetic field ($B=1.5$ T maximum), have also been measured to show the magnetic field dependence.

II. PREPARATION AND CHARACTERIZATION

Two sets of $LaMnO_{3+\delta}$ samples (viz. LaMn–C showing a MIT around 265 K and the other LaMn–S showing no MIT between 350 and 80 K) with different proportions of Mn^{3+}/Mn^{4+} were prepared by ceramic heating route following the procedure mentioned in Ref. 4. The samples $La_{1-x}Pb_xMnO_3$ ($x=0.05-0.5$) were also prepared by the ceramic heating route in a manner similar to our earlier work.[15,16] The x-ray diffraction (XRD) patterns of the samples LaMn–S and LaMn–C are shown in Fig. 1. The conducting sample LaMn–C is found to be fitted with a rhombohedral (with $a=5.477$ Å and $\alpha=60.61°$) or a hexagonal ($a=5.526$ Å and $c=13.355$ Å) structure. These values are comparable with those obtained by other research groups.[4,5] On the other hand, the data of the insulating (semi-

[a]Also at: Department of Physics, Ben-Gurion University of the Negev, P.O. Box 653, Beer-Sheva 84105, Israel.
[b]Electronic mail: sspbkc@mahendra.iacs.res.in

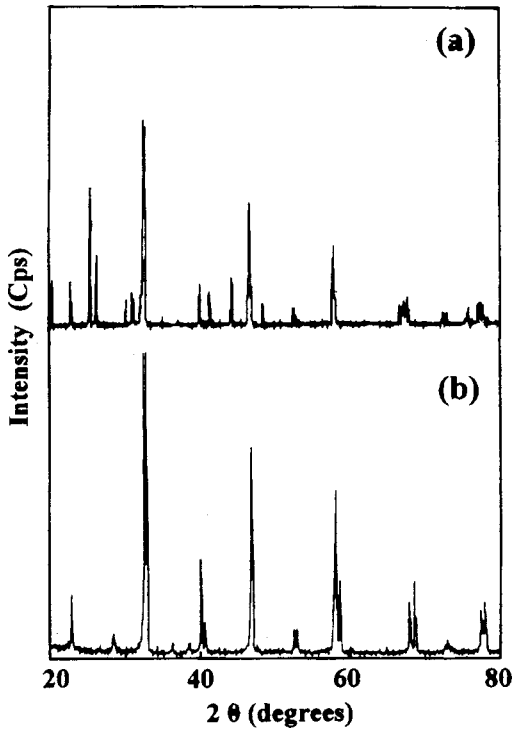

FIG. 1. XRD patterns of two samples (a) LaMn–S without showing a MIT and (b) LaMn–C showing a MIT around 265 K.

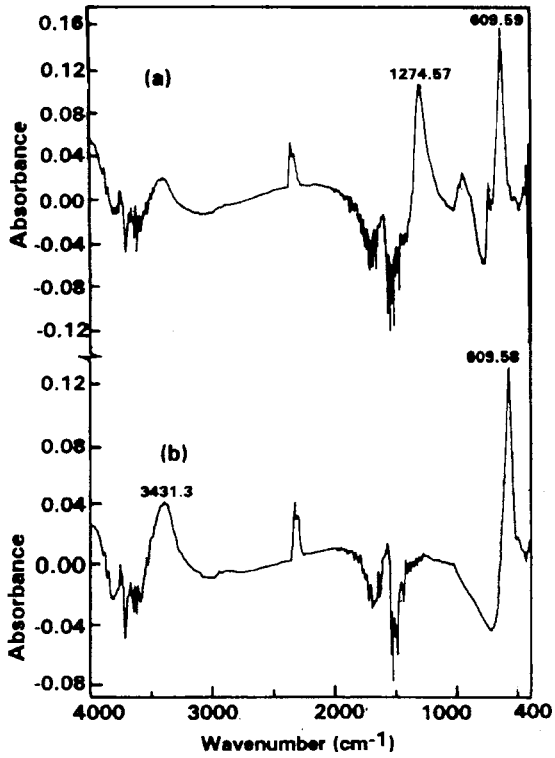

FIG. 2. Infrared spectra of two samples (a) LaMn–S without showing a MIT and (b) LaMn–C showing a MIT around 265 K.

conducting) sample LaMn–S, without showing a MIT, is fitted with an orthorhombic structure. The resistivity of the samples were measured using standard four probe method[15,16] in the temperature range of 80–330 K with an accuracy of ±0.5 K. The infrared spectra of LaMn–S and LaMn–C have been studied to find distinguishing features of the two samples. The infrared spectra of LaMn–C and LaMn–S are shown in Fig. 2.

III. RESULTS AND DISCUSSION

It is seen from the infrared spectra (Fig. 2) that the sample LaMn–S showed an additional peak around 1274.57 cm^{-1}. The peak at about 610 cm^{-1} in both the samples corresponds to the phonon frequency (v_{ph}) of about 1.3×10^{13} Hz. A similar value of v_{ph} is also obtained from fitting the conductivity data (discussed as follows) with the polaron hopping conduction mechanism. Temperature dependent resistivity data shown in Fig. 3(a) indicates that LaMn–S remained semiconducting throughout the temperature range (80–330 K) of our measurements similar to that of La_2CuO_4.[17] All the three set of LaMn–S samples prepared in the same batch showed identical behavior with 1%–2% change of resistivity from each other. The other set of LaMn–C samples, however, exhibited a peak in the resistivity versus temperature curve around the MIT temperature [$T_{mi}=265$ K shown in Fig. 3(b)]. This is the highest T_{mi} reported for the $LaMnO_{3+\delta}$ type sample showing MIT transition.[4] This temperature dependent resistivity behavior is similar to that of the Pb doped LaPbMn–C (inset of Fig. 3). In both the samples LaMn–C and LaPbMn–C, resistivity first increases with decreasing temperature upto T_{mi} (i.e., $d\rho/dT<0$ for $T>T_{mi}$). Hence, the sample is semiconducting above the respective transition temperature ($T_{mi}=265$ and 275 K, respectively, for the LaMn–C and LaPbMn–C). Below this temperature, resistivity decreases with decreasing temperature i.e., $d\rho/dt>0$ for $T<T_{mi}$. The resistivity curves of both the samples (LaMn–C and LaPbMn–C), measured in presence of magnetic field ($B=1.5$ T), are also shown in Fig. 3 which indicated negative magnetoresistance in the presence of a magnetic field. The values of magnetoresistances [$=-(R_H-R_0)/R_0\times 100\%$] for these two samples around MIT are 10% and 14%, respectively. The conductivity data obtained from the present samples in the high temperature (above T_{mi}) range can be interpreted in terms of the polaron hopping conduction theory of Mott[10] based on the strong electron–phonon coupling approximation. The well known[10] expression for small polaron hopping conduction is given by

$$\sigma_{dc}=\sigma_0 \exp(-2R\alpha)[\exp(-W/k_BT)], \quad (1)$$

where $\sigma_0=[v_{ph}Ne^2R^2C(1-C)]/k_BT$. k_B, T, and N are, respectively, the Boltzmann constant, absolute temperature, and the number of ion sites per unit volume. R is the average intersite spacing obtained from the relation $R=(1/N)^{1/3}$ and $C(=Mn^{3+}/Mn_{total})$ is the fraction of sites occupied by a polaron ($C=0.94$, 0.82, and 0.83, respectively, for LaMn–S, LaMn–C, and LaPbMn–C as estimated from magnetic susceptibility and density data). Parameter α is the electron wave function decay constant obtained from fitting the experimental dc conductivity data. v_{ph} is the optical phonon frequency. The activation energy (W) for hopping conduction is given by the relation[14] $W=W_H+W_D/2$ (for $T>\theta_D/2$) and $W=W_D$ (for $T<\theta_D/4$), where W_H is the polaron hop-

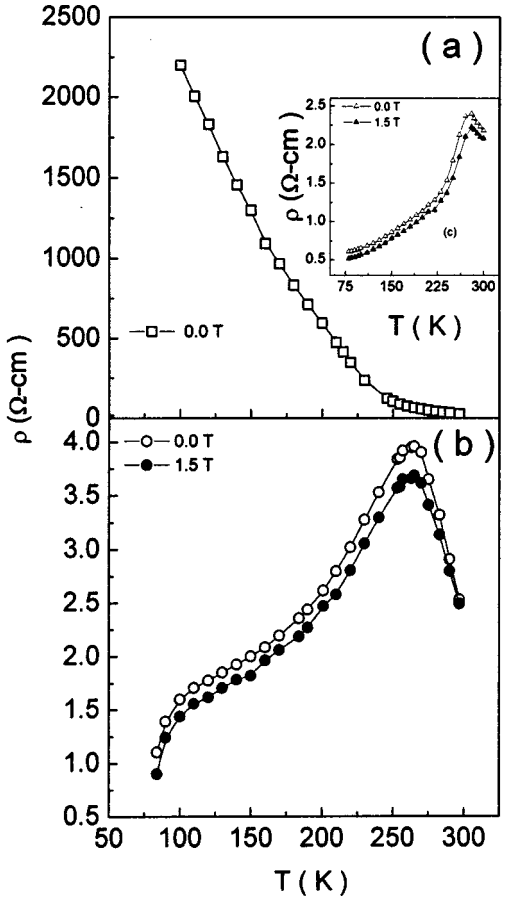

FIG. 3. Thermal variation of resistivity (ρ) of (a) LaMn–S, (b) LaMn–C, and (c) LaPbMn–C (inset) at $B=0$ and $B=1.5$ T magnetic field (for LaMn–C and LaPbMn–C only). Solid lines are guides for the eyes.

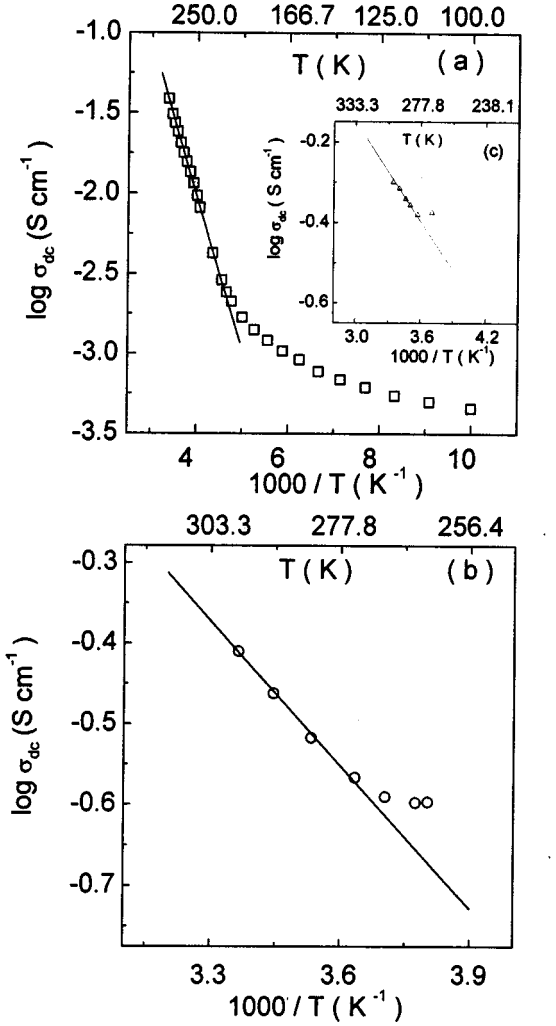

FIG. 4. Variation of $\log \sigma_{dc}$ as a function of inverse temperature $1000/T$ for (a) LaMn–S (b) LaMn–C, and (c) LaPbMn–C. (inset) above the MIT temperature. The solid lines give the best fit to the Mott's Eq. [Eq. (1)] at higher temperatures ($T>T_{mi}$).

ping energy and W_D is the disorder energy. Using the estimated values of R (=5.52, 5.37, and 5.72 Å, respectively, for LaMn–S, LaMn–C, and LaPbMn–C), the hopping energy W_H is calculated from the relation[10]

$$W_H = e^2/4\epsilon_p(1/r_p - 1/R), \tag{2}$$

where $\epsilon_p=(1/\epsilon_s - 1/\epsilon_\infty)$, ϵ_∞, and ϵ_s are the high frequency and static dielectric constants of the samples, and r_p is the polaron radius. The values of ϵ_p are obtained from the dielectric constant measurements of the samples as shown as follows. When the overlap integral between the sites $J_0\exp(-2R\alpha)$ approaches J_0, the hopping is adiabatic, mainly controlled by the activation energy, and the conductivity is given by $\sigma_{dc}=(\sigma_0/T)\exp(-W/k_BT)$. The inverse temperature dependence of $\log\sigma_{dc}$ of the three samples LaMn–S, LaMn–C, and LaPbMn–C are shown in Fig. 4 (for LaMn–C and LaPbMn–C showing MIT, only the semiconducting parts above T_{mi} are plotted). The nonlinear behavior of the logarithm of the dc conductivity indicates a temperature dependence of activation energy which is consistent with the small polaron hopping conduction mechanism exhibited by many semiconducting oxide samples.[10,14,18] Figure 4 predicts temperature dependent activation energy below the respective $\theta_D/2$ values for all the samples. The value of θ_D is estimated from the temperature at which linearity appears in Fig. 4. It is found that for LaMn–C (θ_D =549.83 K with $T_{mi}=265$ K) and LaPbMn–C (θ_D =564.97 K with $T_{mi}=275$ K), the values of θ_D are little higher than that of LaMn–S ($\theta_D=450.7$ K) showing no MIT. The high temperature linear parts of the dc conductivity data (Fig. 4) are well fitted to Eq. (1). The value of W for LaMn–S ($W=211.11$ meV at $B=0$ T) estimated from the slope of the curve in Fig. 4, is however, higher than those of LaMn–C ($W=134.13$, 118.93 meV) at $B=0$ T, and 1.5 T magnetic field) and LaPbMn–C ($W=61.14$, 51.40 meV at $B=0$ T, and $B=1.5$ T). The phonon frequency υ_{ph} ($=0.930\times10^{13}$, 1.14×10^{13}, and 1.17×10^{13} Hz, respectively, for LaMn–S, LaMn–C, and LaPbMn–C, estimated from the relation $h\nu_{ph}=k_B\theta_D$) is close to the optical phonon frequency estimated from infrared spectra of LaMn–S and LaMn–C (Fig. 2) which is of the order of 1.3×10^{13} Hz. Thus, the optical phonon frequency does not differ appreciably in these samples.

The nonzero value of α ($\sim$2.5 nm^{-1}) obtained from fitting the high temperature (linear part in Fig. 4) conductivity data of LaMn–S with Eq. (1) indicated a nonadiabatic hopping conduction mechanism for LaMn–S. But for LaMn–C

and LaPbMn–C showing MIT, the values of σ_{dc} above the respective T_{mi} values can be well fitted to Eq. (1) with $\exp(-2R\alpha)\sim 1$ which indicates adiabatic hopping conduction mechanism. It is, however, always difficult to identify uniquely the nature of hopping conduction mechanism if only the temperature dependence of conductivity is used, because the conductivity subject to the adiabatic small polaron conduction also satisfies the temperature dependence of nonadiabatic hopping conduction. Furthermore, a hopping process of nonadiabatic small polarons requires several restrictions on the electron transfer integral between the neighboring hopping sites. These restrictions are then to be the criteria of judgment whether the hopping conduction is termed adiabatic or nonadiabatic.[19] Other alternative methods to confirm the conduction mechanism in these oxides are discussed as follows.

It is well known[10] that transport in semiconducting oxides can be described by variable range hopping (VRH) of charge carriers. Recently Crespi *et al.*[20] and Jaime *et al.*[21] and Viret[22] also applied VRH conduction mechanism in systems like $Nd_{1-x}(Sr,Pb)_xMnO_3$, La–Ca–Mn–O, etc. at higher temperatures (above 200 K). In the three dimensional cases, the expression for dc conductivity following VRH mechanism can be written as[23]

$$\sigma_{dc}=\sigma_0\exp(-T_0/T)^{1/4}, \tag{3}$$

where T_0 is a constant $[=16\alpha^3/k_BN(E_F)]$ and $N(E_F)$ is the density of states at the Fermi level which can be calculated from the slope of the plot of $\log\sigma_{dc}$ versus $T^{-1/4}$ curves [shown in Figs. 5(a) and 5(b)]. The best fit [solid line in Figs. 5(a) and 5(b)] occurs with $T_0\sim 10^6$ K and $\chi^2\sim 2.71-2.83$ (for different samples, where χ^2 is the weighted sum of the squared deviations). From Fig. 5(a) it is seen that the high temperature (above 180 K) conductivity data of the LaMn–S follow the VRH model [Eq. (3)]. Similarly, for the samples LaMn–C and LaPbMn–C showing MIT, VRH model is applicable above the respective MIT temperatures. From Eq. (3) we obtained $N(E_F)\sim 1.02\times 10^{19}\,\mathrm{eV^{-1}\,cm^{-3}}$ for LaMn–S (using $\alpha=2.5\,\mathrm{nm^{-1}}$ derived from Eq. (1) which is similar to those of many disordered semiconducting transition metal oxides.[18,23] For LaMn–C and LaPbMn–C obeying adiabatic hopping conduction mechanism even above MIT, the dc conductivity data can be fitted with Eq. (3) with $N(E_F)\sim 1.63\times 10^{21}$ and $5.99\times 10^{22}\,\mathrm{eV^{-1}\,cm^{-3}}$, respectively, for LaMn–C and LaPbMn–C. For both the samples we used $\alpha=2.5\,\mathrm{nm^{-1}}$. These values of $N(E_F)$ are comparable to those of $La_{0.7}Ca_{0.3}MnO_3$ $(\sim 4\times 10^{22}\,\mathrm{eV^{-1}\,cm^{-3}}$ with $\alpha=2.22\,\mathrm{nm^{-1}})$ estimated by Coey *et al.*[22] showing MIT. These values of $N(E_F)$ are, however, two orders of magnitude higher than those of LaMn–S and many other disordered semiconducting oxides.[18]

Another attempt has also been made to confirm the nature of hopping conduction for the present samples from the Holstein's condition. According to this condition, the polaron bandwidth J should satisfy the inequality[11] $J>\phi$ (for adiabatic hopping conduction) and $J<\phi$ (for the nonadiabatic hopping conduction) where

$$\phi=(2k_BTW_H/\pi)^{1/4}(h\nu_{ph}/\pi)^{1/2}. \tag{4}$$

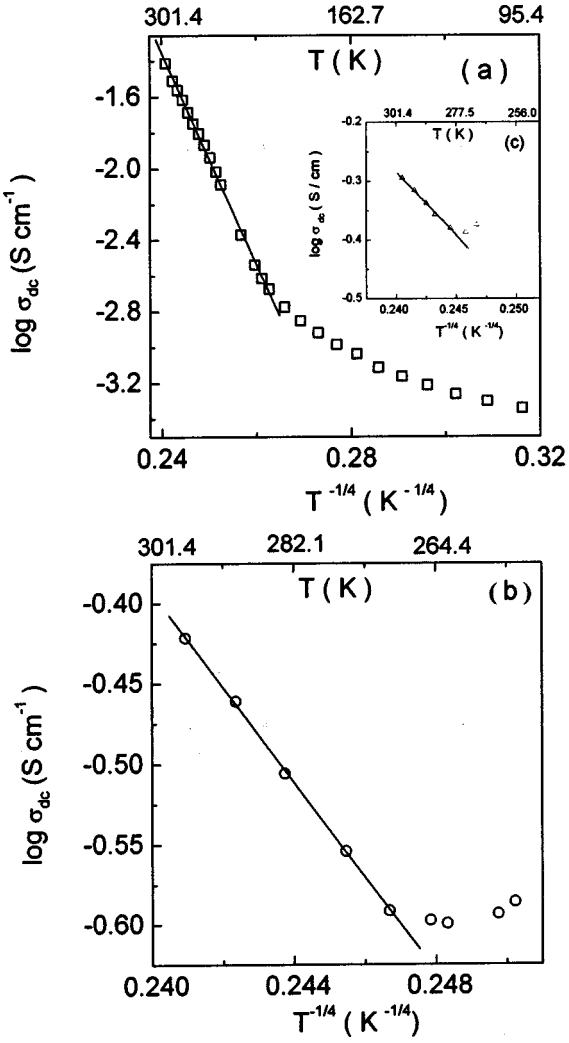

FIG. 5. Variation of conductivity $\log\sigma_{dc}$ as a function of $T^{-1/4}$ for (a) LaMn–S, (b) LaMn–C, and (c) LaPbMn–C (inset) above the MIT temperatures. Solid lines is the best fit to the VRH model [Eq. (3)].

The values of ϕ calculated from Eq. 4 [using the values of $W_H=0.192$, 0.124, and 0.089 eV, respectively, for LaMn–S, LaMn–C, and LaPbMn–C estimated from Eq. (2)] are 2.59×10^{-2}, 2.57×10^{-2}, and 2.39×10^{-2} eV respectively, for LaMn–S, LaMn–C, and LaPbMn–C. Again, the values of J are calculated independently from the model proposed by Mott and Davis[10] viz. $J\sim e^3[N(E_F)/\epsilon_p^3]^{1/2}$. Putting the values of $N(E_F)$, and $\epsilon_p=5.0$ (for LaMn–S), 8.0 (for LaMn–C), and 10.5 (for LaPbMn–C) obtained from dielectric measurement, the independently calculated values of J are 1.56×10^{-2}, 3.08×10^{-2}, 3.93×10^{-2} eV for LaMn–S, LaMn–C, and LaPbMn–C, respectively. Comparing these given values of J and ϕ, it is observed that only for the LaMn–S, without showing MIT, $J<\phi$ (i.e., nonadiabatic hopping condition is strictly satisfied) and for all the doped sample LaMn–C and LaPbMn–C showing MIT, $J>\phi$ (i.e., adiabatic hopping condition is satisfied). Thus, a changeover from the nonadiabatic to the adiabatic hopping conduction mechanism occurs with the appearance of MIT in the rare-earth manganates. This is primarily caused by the change of the ratio Mn^{3+}/Mn^{4+} in the samples.

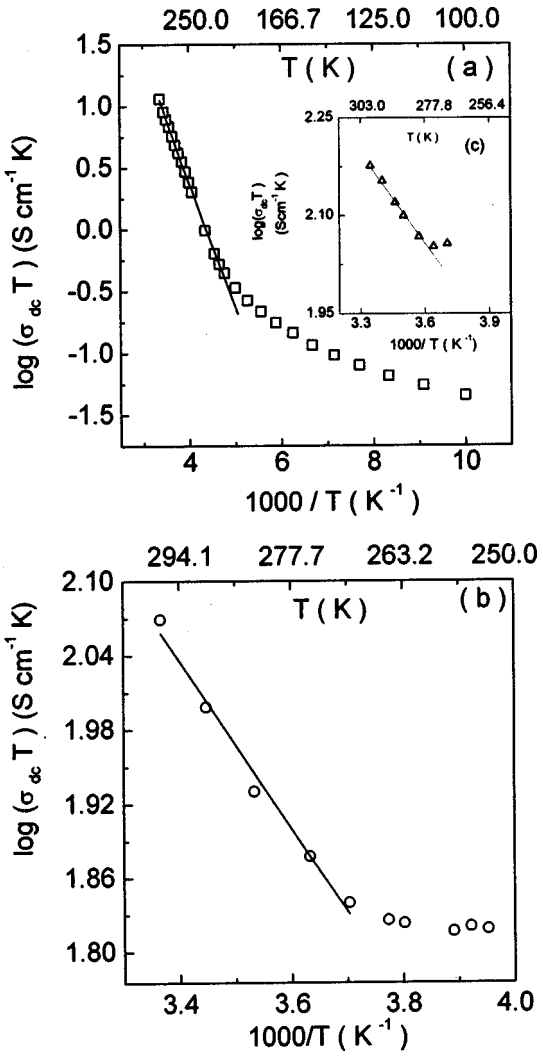

FIG. 6. Plot of $\log(\sigma_{dc}T)$ vs $1000/T$ for (a) LaMn–S, (b) LaMn–C and (c) LaPbMn–C (inset) above the MIT temperature. The solid line corresponds to the best fit curve with Schnakenberg's model [Eq. (5)].

An estimate of the disorder energy W_D and nature of hopping conduction can also be made from the generalized expression of dc conductivity of disordered materials proposed by Schnakenberg.[24] The high temperature conductivity in this model is given by

$$\sigma_{dc}=\sigma_0 T^{-1}[\sinh(h\nu_{ph})]^{1/2}\exp[(-4W_H/h\nu_{ph}) \times[\tanh(h\nu_{ph}\beta/4)]\exp[W_D\beta]. \quad (5)$$

The experimental high temperature conductivity data of all the samples have also been fitted to the Schnakenberg model [Eq. (5)] which give the values of W_D (=0.15, 0.049, and 0.051 eV), W_H=0.18, 0.12, and 0.08 eV, respectively, for LaMn–S, LaMn–C, and LaPbMn–C. The same values of phonon frequencies obtained from fitting the conductivity data with Eq. (1) were used in this fitting. The theoretical best fit curve is shown by the straight line in Fig. 6 (high temperature linear part). This fitting also indicates that the small polaron hopping model is valid for all the samples of our present interest. Using these values of W_H on the right-hand side of Eq. (4), it is again seen that adiabatic hopping condition is valid for the LaMn–C and LaPbMn–C samples while nonadiabatic hopping condition is valid for LaMn–S showing no MIT. Furthermore, disorder energy (W_D previously shown) of LaMn–S is about one order of magnitude higher than those of LaMn–C and LaPbMn–C showing MITs.

It is found that nonadiabatic hopping conduction, in LaMn–S, is also supported by the small polaron hopping model proposed by Emin and Holstein.[11] It may be noted that a small polaron is formed when electron–phonon interaction is strong enough.[11] Following Holstein[11] and Gorham-Bergeron and Emin,[25] the expression for the dc conductivity for nonadiabatic hopping of small polarons in the high temperature ($T>\theta_D/2$) limit can be written as

$$\sigma_{dc}=(Ne^2R^2/6k_BT)(J/h)^2[(\pi/h^2)/2(E_c^{op}+E_c^{ac})k_BT]^{1/2} \times\exp[W_D^2/8(E_c^{op}+E_c^{ac})k_BT]x\exp[-W_D/2k_BT] \times\exp[-E_A^{op}/k_BT-E_A^{ac}/k_BT], \quad (6)$$

where

$$E_c^{op}=E_b^{op}(1/N_p)\Sigma[h\nu_{o,q}/2k_BT]\text{cosech}(h\nu_{o,q}/2k_BT),$$

$$E_c^{ac}=E_b^{ac}(1/N_p)\Sigma[h\nu_{a,q}/2k_BT]\text{cosech}(h\nu_{a,q}/2k_BT),$$

$$E_A^{op}=E_b^{op}(1/N_p)\Sigma[h\nu_{o,q}/2k_BT]\tanh(h\nu_{o,q}/2k_BT),$$

$$E_A^{ac}=E_b^{ac}(1/N_p)\Sigma[h\nu_{a,q}/2k_BT]\tanh(h\nu_{a,q}/2k_BT),$$

$\nu_{o,q}$ and $\nu_{a,q}$ are the optical and acoustical phonon frequencies, respectively, at wave vector q. N_p is the number of phonon modes, E_b^{op} and E_b^{ac} are the polarons binding energies related to optical and acoustical phonons, respectively. Equation (6) has been utilized in calculating the nonadiabatic dc conductivity of the LaMn–S system, assuming that the acoustic phonon density of states is approximately given by $g(\omega)\propto\omega^2$ and that the mean optical phonon frequency, ν_{ph} is constant. Using the value of W_D obtained from the Schnakenberg model [Eq. (5)] as discussed, the high temperature conductivity data of LaMn–S were fitted with parameters $E_c^{ac}(\text{eV})\times10^2=3.9$, $E_c^{op}(\text{eV})\times10^2=3.9$, $E_a^{ac}(\text{eV})\times10^2=7.50$, and $E_a^{ac}(\text{eV})\times10^2=7.50$. The observed good fitting of the conductivity data with Eq. (6) again supports the validity of nonadiabatic hopping conduction mechanism in LaMn–S showing no MIT. Similar calculations can also be extended to show the adiabatic hopping conduction mechanism followed by the corresponding LaMn–C and LaPbMn–C showing MITs. Since no other theoretical or experimental data are available to compare the model parameters estimated from this Eq. (6), we did not proceed to make such calculations for other samples.

An attempt has also been made to calculate the small polaron coupling constant γ_P, which is a measure of electron–phonon interaction in these samples, using the relation[10,14] $\gamma_P=2W_H/h\gamma_{Ph}$. For LaMn–S, the estimated value of $\gamma_P(=9.28)$ is greater than 4 which indicates[14] stronger electron–phonon interaction in LaMn–S than those of LaMn–C and LaPbMn–C showing MIT with $\gamma_P=5.05$ and 3.28, respectively. A strong electron–phonon interaction also supports the theory of Jahn–Teller distortion proposed by Milles *et al.*[26] The lattice polaronic effects due to strong

electron–phonon coupling (arising from strong Jahn–Teller effect) should be involved in this type of materials showing MIT, which is supported by the present work.

It is to be noted here that much of the behavior of resistivity $\rho(T)$ above the magnetic transition is indicative of conduction by magnetic polarons.[20,27] In fact, a magnetic polaron consists of an electron which polarizes the magnetic moments of the ions around the transition, forming in effect a small ferromagnetic region. Magnetic polarons are localized as a consequence of magnetic interactions, so that conduction proceeds via thermal hopping. This also explains the activated behavior of the resistivity above the MIT in LaMn–C and LaPbMn–C. Magnetic polarons, however, can exist only over a limited range of temperature and magnetic field close to the onset of ferromagnetism. At zero field, the formation of magnetic polarons will not be possible if the magnetic ions are ferromagnetically ordered, so that the hopping conduction behavior will not occur in the samples as the temperature is lowered below the magnetic ordering temperature. This explains the rapid fall of resistivity below this ordering temperature.[28] Likewise, an increase of external magnetic field will increase the ferromagnetic order so that formation of magnetic polarons will be inhibited.[29,30] The paramagnetic state (above and around the MIT temperature) is considered to be the environment for the formation of magnetic polarons. Since both LaMn–C and LaPbMn–C are paramagnetic above the MIT temperatures, magnetic polarons can survive in this regime of temperature. Like field dependent resistivity, thermoelectric power of LaMn–C and LaPbMn–C, in presence of magnetic field ($B=1.5$ T), showed appreciable field dependence (Figs. 7 and 8) and hence indicated the presence of magnetic polaron.[27] It is seen from Figs. 7 and 8 that the magnetic field dependent thermoelectric power of LaMn–S, LaMn–C, and LaPbMn–C exhibits some interesting features. For the sample LaMn–S [Fig. 7(a)], field dependent Seebeck coefficient (S_H) is less than that of the corresponding zero field value (S_0) for the entire range of temperature. On the other hand, for LaMn–C and LaPbMn–C [Figs. 7(b) and 7(c)], above the MIT (or magnetic ordering temperature), $S_H<S_0$ but below or around MIT ($\sim$265 K) there is a changeover in the magnitude of S_0 and S_H (i.e., S_H becomes $>S_0$). Such a changeover of the S values is not observed in LaMn–S without showing MIT [Fig. 7(a)]. It is also to be noted that above the MIT temperature, the TEP values of LaMn–C are negative while those of the Pb-doped LaPbMn–C are always positive. Moreover, below and around MIT, appreciable decrease of the TEP under magnetic field is observed in LaPbMn–C (down to $\sim$120 K). This decrease is very small in case of the undoped sample LaMn–C showing MIT. An appreciable change of S under magnetic field is considered to be associated with magnetic polarons. The broad peak in the temperature dependent TEP data [Figs. 7(b) and 7(c)] around 150 K in both LaMn–C and LaPbMn–C might be due to some form of localization caused by magnetic ordering of La ions and this region needs further investigation.

Since the high temperature region transport is governed by thermally activated polarons, we have also tried to fit the high temperature TEP data with Mott's equation[20,31]

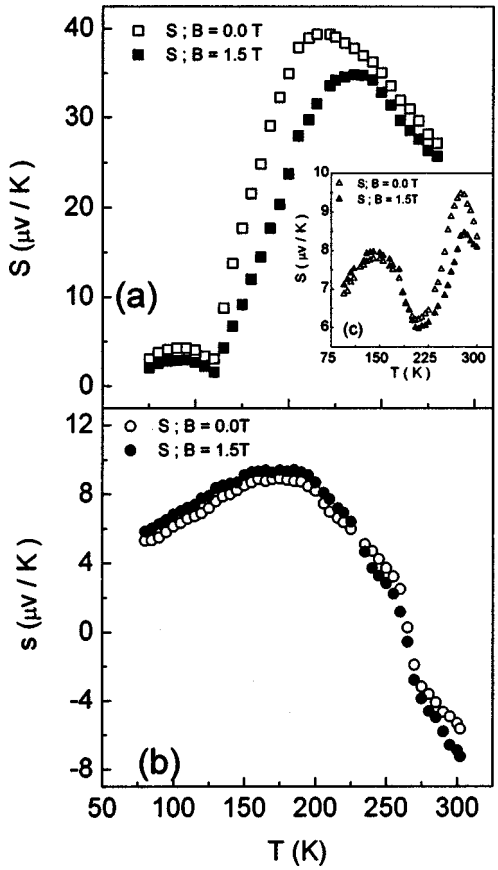

FIG. 7. Thermoelectric power (S) of (a) LaMn–S, (b) LaMn–C, and (c) LaPbMn–C at $B=0$ and $B=1.5$ T magnetic field.

$$S=k_B/e(E_s/k_BT+\alpha'), \tag{7}$$

where k_B is Boltzmann constant, e is electronic charge, and α' is a constant of proportionality between heat transfer and kinetic energy of electrons or holes. For $\alpha'<1$ small polaronic hopping transport occurs.[32,33] For $\alpha'>2$ conduction is due to the large polarons.[13,14] From fitting the high temperature TEP data (linear part in Fig. 8), the values of α' are found to be 0.393, 0.418, and 0.071, respectively, for LaMn–S, LaMn–C, and LaMPb–C indicating small polaron hopping condition valid for these samples. From the slope of S versus $1/T$ curve (Fig. 8), the estimated values of activation energy E_s are 17.19, 8.52, and 4.36 meV, respectively, for LaMn–S, LaMn–C, and LaPbMn–C in zero field ($B=0$ T) and the corresponding values in presence of magnetic field ($B=1.5$ T) are 18.22, and 10.89 meV for LaMn–S and LaMn–C, respectively. Generally W (activation energy obtained from resistivity curve) is greater than E_s and the nonequivalence of W and E_s confirms that charge transport is mostly dominated by thermally activated hopping of carriers.[20,30] This causes[21] the experimental activation (W) energies measured from resistivity and thermoelectric power to differ[21] with $W_H=W-E_s$ ($=$193.91, 125.61, and 56.79 meV for LaMn–S, LaMn–C, and LaPbMn–C, respectively). Interestingly, these values of W_H are close to those estimated from Eq. (2) and also from the aforementioned Schnakenberg's Eq. (5). Since an external field will increase the ferromagnetic order, prominent negative magnetoresistance and

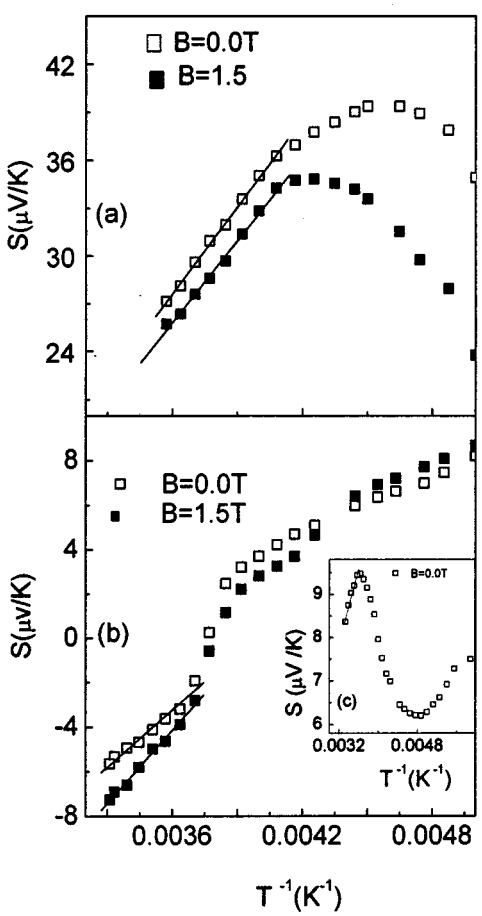

FIG. 8. Plot of thermoelectric power (S) vs $1/T$ of (a) LaMn–S, (b) LaMn–C [for $B=0$ T and 1.5 T], and (c) LaPbMn–C (for $B=0$). The linear part (solid line), above the MIT temperature, shows the best fit curve with the Mott's Eq. (7).

lowering of the activation energy W are observed. For LaMn–C, for example, $W=134.13$ meV, in absence of field and 118.93 meV at $B=1.5$ T already mentioned.

IV. CONCLUSION

The $LaMnO_{B+\delta}$ type samples showing semiconductor to metallic transition followed adiabatic hopping conduction mechanism while the similar samples showing no semiconductor–metal transition followed nonadiabatic hopping mechanism. Such a change of conduction mechanism is associated with the change of the ratio $C(=Mn^{3+}/Mn^{3+}+Mn^{4+})$, Debye temperature, electron–phonon interaction constant, disorder energy, etc. Though the variable range hopping model is found to be valid for the present samples of our investigation and also for similar other samples reported by different groups[20,21] (above the MIT temperatures), the density of states at the Fermi level $N(E_F)$ comes out to be larger than those of the LaMn–S (showing no MIT) and many other oxide semiconductors. However, for the LaMn–S oxide, the $N(E_F)$ value agrees with those of many semiconducting oxide systems.[23] The electron–phonon interaction in LaMn–S is higher than those of the samples showing MITs. Field dependence of thermoelectric power is consider to be associated with the presence of magnetic polarons in the present samples. However, further investigation is necessary to explain the anomalous behavior of the thermoelectric power of the samples in presence of a magnetic field.

ACKNOWLEDGMENT

The authors are grateful to the Department of Science and Technology, Government of India, for financial support to carry out this work. The authors are also grateful to Professor S. P. Sengupta, Materials Science Department, IACS, for going through the manuscript.

[1] R. Senis, B. Martinez, J. Fontcuberta, X. Obradors, W. Cheikh-Rouhou, P. Strobel, C. B. Chaillout, and M. Perrnet, J. Appl. Phys. **85**, 5405 (2000).
[2] A. Asamitsu, A. Morotomo, Y. Tomioka, T. Arima, T. Tokura, and Y. Tokura, Nature (London) **373**, 407 (1995).
[3] C. T. Lin, Y. Yan, E. Bischoff, K. Peters, and E. Schonherr, J. Appl. Phys. **85**, 5393 (1999).
[4] J. Topfer and J. B. Goodenough, Solid State Chem. **130**, 117 (1997).
[5] R. Mahendiran, S. K. Tiwary, A. K. Roychaudhuri, T. V. Ramakrishnan, R. Mahesh, N. Rangavittal, and C. N. R. Rao, Phys. Rev. B **53**, 3348 (1996).
[6] J. M. D. Coey, M. Viret, and S. von Molnar, Adv. Phys. **48**, 167 (1999).
[7] B. Chen, A. G. Rojo, C. Uher, H. L. Ju, and R. L. Greene, Phys. Rev. B **55**, 15471 (1997).
[8] R. Mahesh, R. Mahendiran, A. K. Roychaudhuri, and C. N. R. Rao, Solid State Chem. **120**, 204 (1995).
[9] C. Zener, Phys. Rev. **82**, 405 (1951).
[10] N. F. Mott and E. A. Davis, in *Electronic Processes in Noncrystalline Materials* (Clarendon, Oxford 1971).
[11] T. Holstein, Ann. Phys. (N.Y.) **8**, 343 (1959).
[12] S. Wang, K. Li, Z. Chen, and Y. Zhang, Phys. Rev. B **61**, 575 (2000).
[13] J. Appel, Solid State Phys. **21**, 193 (1968).
[14] G. N. Austin and N. F. Mott, Adv. Phys. **18**, 41 (1969).
[15] E. Rozenberg, G. Gorodetski, N. Froumi, J. Pelleg, M. Polak, and B. K. Chaudhuri, J. Phys. (France) **8**, 359 (1998).
[16] A. I. Shames, E. Rozenberg, G. Gorodetski, J. Pellegand, and B. K. Chaudhuri, Solid State Commun. **107**, 91 (1998).
[17] P. Lukenheimer, M. Resch, and A. Loidl, Phys. Rev. Lett. **69**, 498 (1990).
[18] S. R. Elliott, *Physics of Amorphous Materials* (Longmans, London, Green, 1983), p. 291.
[19] N. Nakamura and E. Eguchi, Solid State Chem. **145**, 58 (1999).
[20] V. H. Crespi, Li Lu, Y. X. Jia, K. Khazeni, A. Zetll, and M. L. Cohen, Phys. Rev. B **53**, 14303 (1996).
[21] M. Jaime, M. B. Salamon, K. Pettit, M. Rubinstein, R. E. Trece, J. S. Horwitz, and D. B. Chirisoy, Appl. Phys. Lett. **68**, 1576 (1996).
[22] M. Viret, L. Ranno, and J. M. D. Coey, Phys. Rev. B **55**, 8067 (1997); and references therein.
[23] N. F. Mott, J. Non-Cryst. Solids **1**, 1 (1968).
[24] J. Schnakenberg, Phys. Status Solidi **28**, 623 (1968).
[25] E. Goroham-Bergeron and D. Emin, Phys. Rev. B **15**, 3667 (1977).
[26] A. J. Milles, B. I. Shraiman, and R. Mueller, Phys. Rev. Lett. **77**, 175 (1996).
[27] R. M. Kusters, J. Singleton, D. A. Keen, R. Mcgreevy, and W. Hayes, Physica B **155**, 362 (1989).
[28] Y. Shapira, S. Foner, N. F. Oliveira, and T. B. Reed, Phys. Rev. B **10**, 4765 (1974).
[29] S. Washburn, R. A. Webb, S. von Molnar, F. Holtzberg, G. Flouque, and G. Remenyi, Phys. Rev. B **30**, 6224 (1984).
[30] M. J. Gillan and D. Wolf, Phys. Rev. Lett. **55**, 1299 (1985).
[31] M. Jaime, K. Salamon, M. Rubinstein, R. E. Trece, J. S. Horwitz, and D. B. Chirisoy, Phys. Rev. B **54**, 11914 (1996).
[32] H. Sakata, T. Kikuchi, H. H. Qiu, H. Shimizu, and M. Amano, J. Mater. Sci.: Mater. Electron. **10**, 643 (1999).
[33] A. Mansingh and A. Dhawan, J. Phys. C **11**, 3439 (1978).